Measuring electrostatic, van der Waals, and hydration forces in electrolyte solutions with an atomic force microscope

Hans-Jürgen Butt
Max-Planck-Institut für Biophysik, Kennedyallee 70, 6000 Frankfurt a. M. 70, Germany

ABSTRACT In atomic force microscopy, the tip experiences electrostatic, van der Waals, and hydration forces when imaging in electrolyte solution above a charged surface. To study the electrostatic interaction force vs distance, curves were recorded at different salt concentrations and pH values. This was done with tips bearing surface charges of different sign and magnitude (silicon nitride, Al_2O_3, glass, and diamond) on negatively charged surfaces (mica and glass). In addition to the van der Waals attraction, neutral and negatively charged tips experienced a repulsive force. This repulsive force depended on the salt concentration. It decayed exponentially with distance having a decay length similar to the Debye length. Typical forces were about 0.1 nN strong. With positively charged tips, purely attractive forces were observed. Comparing these results with calculations showed the electrostatic origin of this force.

In the presence of high concentrations (>3 M) of divalent cations, where the electrostatic force can be completely ignored, another repulsive force was observed with silicon nitride tips on mica. This force decayed roughly exponentially with a decay length of 3 nm and was ~0.07-nN strong. This repulsion is attributed to the hydration force.

INTRODUCTION

The atomic force microscope (AFM), invented by Binnig, Quate and Gerber (1986), has become an important tool for imaging surfaces (Wickramasinghe, 1989). In the AFM a sharp tip at the end of a cantilever is scanned over a surface. While scanning, surface features deflect the tip and thus the cantilever. By measuring the deflection of the cantilever a topographic image of the surface can be obtained.

Many AFM studies were done in aqueous medium. This is for two reasons. The force applied by the tip to the surface can be reduced by a factor of 10–100 compared to the force in air as the meniscus force is absent (Weisenhorn et al., 1989). Second, for many applications, water is the natural environment. Biological materials for instance often denature if not kept in electrolyte solution.

To interpret AFM images correctly it is necessary to know which forces are acting between tip and surface. In addition, knowledge about the different components of the force is important to minimize the total force and thus prevent possible deformation or destruction of the sample. When imaging in water, different forces act between tip and sample (Burnham and Colton, 1991; Lindsay, 1991). The AFM is based on the repulsive force coming from overlapping electron orbitals between tip and sample atoms. Another interaction is the van der Waals attraction. The van der Waals (vdW) force has been calculated (Albrecht, 1989; Girard et al., 1989; Goodman and Garcia, 1991; Hartmann, 1991) and measured (Burnham and Colton, 1989; Mate et al., 1989; Burnham et al., 1990; Weisenhorn et al., 1991) for different tip-medium-sample combinations.

In aqueous medium, the electrostatic force should be considered. In water, many surfaces are charged. The charging of surfaces can come about in two ways: by the dissociation of surface groups (e.g., the dissociation of protons from carboxylic groups), or by the adsorption of ions onto the surface. These surface charges cause an electric field which decreases roughly exponentially with increasing distance from the surface (McLaughlin, 1977). Even if the tip does not bear free electric charges, polarization charges at the tip/electrolyte interface caused by the electric field give rise to an electrostatic interaction. An additional effect is the osmotic pressure acting on the tip. Surface charges attract counterions and the overall ion concentration increases near the sample. These ions cause an osmotic pressure which repels the tip.

Based on an equation by Parsegian and Gingell, 1972, the electrostatic force on a sphere with radius R was approximated for surface potentials below 50 mV (Butt, 1991):

$$F_e = \frac{2\pi\lambda_D R}{\epsilon_0\epsilon} \cdot [(\sigma_T^2 + \sigma_S^2) \cdot e^{-2D/\lambda_D} + 2\sigma_T\sigma_S \cdot e^{-D/\lambda_D}]. \quad (1)$$

σ_T and σ_S are the surface charge densities of tip and sample surface, ϵ_0 and ϵ represent the vacuum permittivity and the dielectric constant of water. D is the distance between tip and sample surface. λ_D is the Debye length.

0006-3495/91/12/1438/07 $2.00

For a monovalent salt and at 22°C it is given by

$$\lambda_D = \frac{0.304}{\sqrt{C}} \text{ nm.} \quad (2)$$

C is the bulk concentration of the salt in mol/l. To obtain Eq. 1, it was assumed that $R \gg \lambda_D$ and $e^{D/\lambda_D} \gg e^{-D/\lambda_D}$. For a neutral tip above a charged surface numerical calculations showed that the electrostatic force should be repulsive and $10^{-12} - 10^{-10}$ N strong (Butt, 1991). First experiments confirmed the existence of an electrostatic force (Weisenhorn et al., 1991).

Another force acting between interfaces in water is the hydration force. When Pashley and Israelachvili (Pashley, 1981*a* and *b*; Israelachvili and Pashley, 1983; Pashley and Israelachvili, 1984) measured the force between two mica surfaces in electrolyte, they found, in addition to the electrostatic and vdW force, a short-range repulsive force at higher salt concentrations. This repulsion varied with the type of cation in solution. The more hydrated cations such as Mg^{2+} and Ca^{2+} gave stronger repulsive forces than the less hydrated monovalent ions such as K^+ and Cs^+. These features led Pashley, 1981*a*, to suggest that the repulsive force was due to the work required to dehydrate the adsorbed ions on forcing the mica sheets together.

In this paper I describe measurements of the electrostatic and hydration force. To study the electrostatic interaction force vs distance curves were measured between neutral and negatively charged tips and negatively charged surfaces. In addition to the vdW attraction, a repulsive force was observed which depended on the salt concentration. This force decayed roughly exponentially with a characteristic decay length similar to the Debye length, indicating its electrostatic origin.

In another series of experiments, the force between an alumina (Al_2O_3) tip and mica was measured at different pH values. At high pH alumina and mica are negatively charged and a repulsive force was observed. At low pH, where alumina is positively charged and mica is negative, a pure attractive force was measured.

At very high concentrations of divalent cations (>3 M) a short range repulsive force was measured between a silicon nitride tip and a mica surface. This force is attributed to the hydration force.

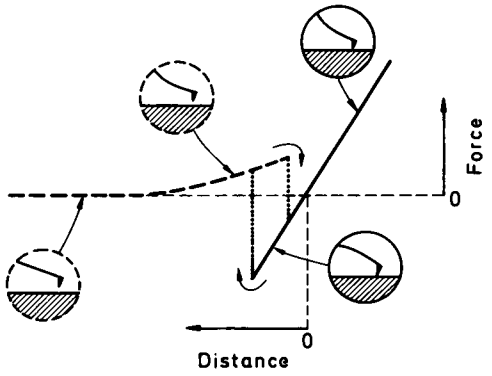

FIGURE 1 Schematic of a typical force vs distance curve. The vertical axis in Fig. 1 represents the force acting between tip and sample surface. It is obtained by multiplying the deflection of the cantilever with its spring constant. The horizontal axis represents the distance the sample is moved up and down by the *xyz* translator. When going to the right the sample approaches the tip. A cycle in the force versus distance curve starts at a large tip-surface separation on the left side of the diagram in the nontouching regime (*dashed line*). In the schematic it was assumed that first a repulsion acts between tip and sample. Hence, when the sample approaches the tip the cantilever bends upwards. At a certain point, the tip jumps onto the surface. This jump in occurs when the gradient of the vdW attraction exceeds the gradients of the spring and repulsive force. Moving the sample still further causes a deflection of the cantilever of the same amount the sample is moved. This is represented by the diagonal continuous line where the tip touches the sample. Finally, the sample is retracted again and brought back to its starting position. When the sample is moved away from the tip, the tip sticks to the surface up to large distances. This is caused by the vdW force and by adhesion. Due to this hysteresis, repulsive forces are more difficult to observe on the way out than on the approach.

MATERIALS AND METHODS

A commercial AFM (Digital Instruments, Santa Barbara, CA) including control electronics and software (for details see Gould et al., 1990) was used to measure force versus distance curves. A force versus distance curve (Fig. 1) displays the deflection of the cantilever, on which the tip is mounted, as a function of the vertical position of the *xyz* translator, on which the sample is mounted. The *xyz* translator moves the sample up and down with constant speed (except at the turning points). This movement is induced by applying a voltage to the piezoelectric element which is responsible for the *z* direction. The total time for a complete up and down cycle was ~1 s.

To record force vs distance curves, the deflection signal and the *z* voltage of the *xyz* translator were fed into two channels of a digital oscilloscope. Averaged signals were later transferred to a computer and the approaching part of force versus distance curves was further analyzed.

As samples, freshly cleaved mica (G.S.I. ruby mica, Plano W. Planet GmbH, Marburg, Germany) or microscope cover glasses (Assistent, Kühn und Bayer, Nidderau, Germany) were used. The glass was cleaned with 37% HCl for 20 h at room temperature. In addition, flat polished diamond pieces with an area of ~2 × 2 mm were mechanically attached to teflon discs. In this way it was possible to clean the diamond before each experiment with 37% HCl for 1 h. Silicon nitride chips were glued with water insoluable epoxy (Bindulin 2-Komp.-Reaktionskleber, Bindulin, Fürth, Germany) to microscope cover glasses. These cover glasses and the teflon discs were glued to steel discs to mount the samples on the piezoelectric scanner.

The tips were microfabricated silicon nitride tips (NANOPROBES, Digital Instruments, Santa Barbara, CA), shards of alumina ($\gamma - Al_2O_3$, Aldrich Chemical Co., Steinheim, Germany) or diamond (Strauss, Frankfurt, Germany), or glass beads (Roth GmbH, Karlsruhe, Germany). Shards of alumina were obtained by crushing pieces between two hardened steel plates. Alumina and diamond shards (~50 μm)

and the glass beads (diameter of 120 ± 10 μm) were glued on a cantilever with water insoluble epoxy (BINDULIN 2-Komp.-Reaktionskleber). The relatively large size of the tip was chosen to prevent epoxy from going on the imaging side of the tip. All materials were cleaned in 37% HCl for 1 h before gluing them onto cantilevers. The cantilevers were 200-μm long and had a spring constant of 0.032 N/m or 0.064 N/m (Digital Instruments). All silicon nitride tips and two of the three diamond tips used gave molecularly resolved images of mica.

Chemicals were grade p.a. and bought from Fluka Chemical Corp. (Buchs, Switzerland), E. Merck (Darmstadt, Germany), Roth GmbH (Karlsruhe, Germany), or Sigma Chemical Co. (St. Louis, MO). The water was deionized (resistivity: 18 MΩ cm). The following buffers were used: Citric acid (pH 3.1 and 4.6), 2-[N-Morpholino]ethanesulfonic acid (pH 6.1), Imidazole (pH 7.1), Tris-(hydroxymethyl)-aminomethan (pH 8.1), 2[N-Cyclohexylamino]ethanesulfonic acid (pH 9.3), and 3-[(3-Cholamidopropyl)dimethyl-ammonio]-1-propane sulfonat (pH 10.4).

RESULTS AND DISCUSSION

Height calibration

The z calibration of the xyz translator was controlled in two ways. First, purple membranes were imaged and their thickness of 4.9 nm was used as a standard (see Butt et al., 1991). Second, the xyz translator was calibrated by imaging an inclined plane. Therefore, a 5 × 5 mm piece of a microscope cover glass was glued onto a steel disc at an inclination angle of ~15°. The inclination angle α was measured with a stereo microscope. The lateral movement of the xyz translator was calibrated by imaging the hexagonal lattice of mica and by imaging optical diffraction gratings. Then the inclined plane was imaged over a certain scan area $\Delta x \times \Delta y$. If the plane is inclined only in the x direction, the expected difference in the z direction Δz is $tg\alpha \cdot \Delta x$. The calibration with purple membranes gave 10% bigger values for $\Delta z/\Delta V_z$ (ΔV_z is the voltage applied to the z piezo of the xyz translator) than calibrating with the inclined plane.

Force versus distance curves at different salt concentrations

Fig. 2 shows a series of force vs distance curves measured with a silicon nitride tip on mica. The curves were obtained at KCl concentrations between 0.5 mM and 100 mM. At 0.5 mM a repulsive force of ~0.13 nN can be seen which decays with increasing distance between tip and surface. The jump-in due to the vdW attraction occurred very close to the surface (≈1 nm) and is barely visible. In some experiments, no jump in occurred at all. With increasing salt concentration three things happened: The repulsive force decreased, its decay became steeper, and the vdW attraction became clearly visible. At 100 mM, only the vdW attraction and no repulsion was observed.

Force versus distance curves measured in deionized water looked like the curve obtained in 100 mM salt; no repulsion and a large jump-in distance was observed. The reason is that the decay length is so large that it is impossible to distinguish the decaying force from the zero force line. The jump in occurs at a distance where the force gradient of the vdW attraction exceeds the force gradients of the spring force and the electrostatic repulsion (Burnham et al., 1990). For deionized water, the gradient of the electrostatic force is low and the tip jumps onto the surface at large distances.

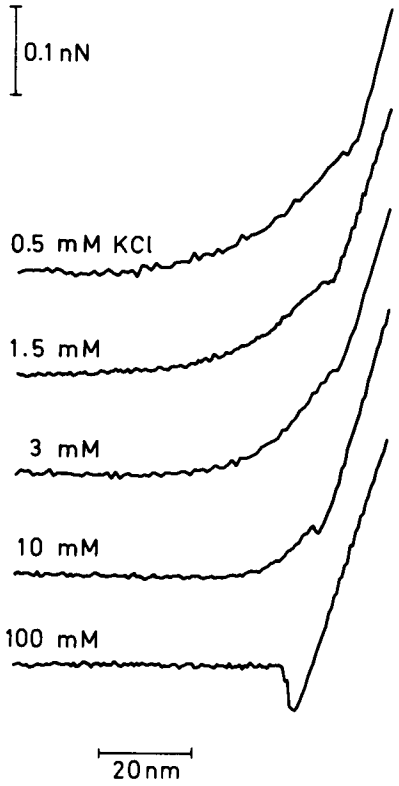

FIGURE 2 Force versus distance curves measured at different KCl concentrations with a silicon nitride tip on mica. The pH was ≈6 due to dissolved CO_2. All curves were 16 times averaged. Only the approach of the sample to the tip is shown.

Measurements like the one shown in Fig. 2 were also done with diamond on mica and glass beads on glass. The same behavior was observed in all cases. When extrapolating the repulsive force to zero distance the average force at 3 mM KCl was 0.12 nN for silicon nitride on mica, 0.07 nN for diamond on mica, and 0.4 nN for glass beads on glass. These results can be compared with values expected from Eq. 1 for a neutral tip on mica. The surface charge density of mica in 3 mM KCl is -0.009 C/m^2 (Pashley, 1981*a*). From AFM images of silicon nitride tips, the radius of curvature was estimated to be ~15 nm. Then, Eq. 1 predicts a force of 0.06 nN. The good agreement between experiment and

calculation should not be over-valued. Measured force amplitudes varied by a factor of two to three for different series of experiments. This is probably mainly due to different tip shapes and different radii of curvature. In addition, to derive Eq. 1, it was assumed that $e^{D/\lambda_D} \gg e^{-D/\lambda_D}$. Hence, in a strict sense Eq. 1 is not valid for $D \rightarrow 0$.

To quantify the characteristic range of the repulsive force and to compare the experiments with calculations, I tried to fit the repulsive part of the force versus distance curves with the exponential function $A \cdot e^{-D/\lambda}$. λ, the decay length, and A, the amplitude, were the fitting parameters. Only distances >3 nm from the jump-in point of the touching regime of the force versus distance curve were considered in the fitting procedure.

The repulsive parts of all force versus distance curves could be fitted with the exponential function. Fig. 3 shows the obtained decay lengths versus the inverse of the square root of the salt concentration C. For all tip-sample combinations the decay length increased for decreasing salt concentration. Within the error of the measurements measured decay lengths were similar to the Debye length (*dashed line* in Fig. 3).

A decay length similar to the Debye length was predicted by the second term in Eq. 1. The first term in Eq. 1 describes an exponential decay with a decay constant of $\lambda_D/2$. σ_T, σ_S, and the distance D determine which term dominates the decay of the electrostatic force. If the surface charge densities are very different, e.g., the tip is neutral, the first term dominates. If $\sigma_T \approx \sigma_S$ the second term controls the decay. From Eq. 1 follows that for distances D larger than

$$\lambda_D \cdot Ln\left(\frac{\sigma_T^2 + \sigma_S^2}{2\sigma_T\sigma_S}\right),$$

the second term dominates. Practically, the first term contributes to the expected decay length only if one surface charge is very much different from the other. If for instance, σ_T is only one third of σ_S, the second term is already bigger than the first term for distances $>0.5\lambda_D$. As for fitting only the signal of distance >3 nm away from the jump-in point were used, the contribution of the first term can easily be overlooked.

For glass beads on glass, tip and sample surface bear negative surface charges densities ($\sigma_T \approx \sigma_S$) and the decay length should be equal to the Debye length (*dashed line* in Fig. 3). This was observed.

In the case of diamond on mica or silicon nitride on mica the result was surprising. Both materials were expected to be neutral ($\sigma_T = 0$). Then, the second term in Eq. 1 can be neglected and values predicted by Eq. 1 are a factor two smaller than the measured decay lengths. However, when measuring the force between silicon nitride tips and silicon nitride samples or diamond tips and diamond samples a repulsive force component was observed above pH 9. At neutral pH sometimes a repulsive force was observed but often the vdW attraction was too strong to measure the repulsion. Still, these measurements indicate that diamond and silicon nitride bear a slight negative surface charge. Silicon nitride for example might form an oxide layer on the surface. Silicon oxide has hydroxyl groups on its surface which would give rise to a negative surface charge. In this case, a decay length similar to the Debye length is expected.

A possible influence of the vdW attraction on the shape of the repulsive part of the force curve was tested. The vdW attraction is proportional to $1/D^{1...2}$ (Israelachvili, 1985; Burnham and Colton, 1989; Hartmann, 1991). Though all curves could be fitted with a single exponential and no $1/D^{1...2}$ function was necessary, an influence of the vdW attraction on the obtained decay lengths can not be excluded. The true distance deviates from the measured distance due to the interaction between tip and sample surface. When the *xyz* translator moves the sample towards the tip, electrostatic forces repel the tip and the cantilever bends away from the sample. Hence, the distance between tip and sample is larger than the distance expected from measuring the applied z voltage. However, taking this effect into account in the fitting procedure did not change the resultant decay lengths significantly.

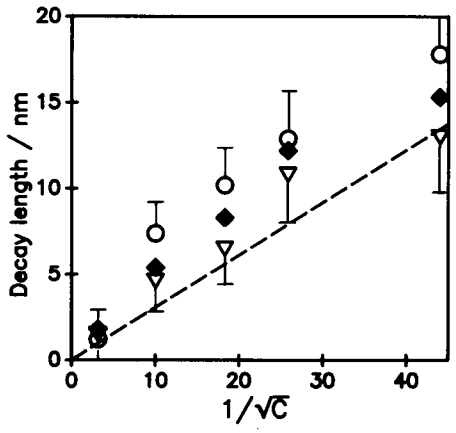

FIGURE 3 Decay lengths versus the inverse of the square root of the KCl concentration (in M). Experiments were done with glass beads on glass (*open spheres*), diamond shards on mica (*filled diamonds*), and silicon nitride on mica (*open triangles*). The pH was ~6 (diamond and silicon nitride) or ~9 (glass beads). The dashed line represents the Debye length. The error of the decay length is indicated for the experiments with glass beads and silicon nitride tips.

pH dependency of the force between an alumina tip and mica

Fig. 4 shows force vs distance curves obtained with an alumina tip on mica at different pH values. All electrolyte solutions contained 2 mM KCl. At pH 10.4, a strong repulsive force was measured. When lowering the pH the repulsive force decreased. From pH 7.1 on no repulsive force was observed anymore. At even lower pH the force became more and more attractive.

This variation of the force with changing pH can be explained with the electrostatic and vdW force. The vdW attraction is independent on pH, but the electrostatic force changes as the surface charge of alumina changes with pH. At pH 8.1, alumina is not charged. Below this point of zero-charge alumina is positive, above pH 8.1, it is negatively charged (Huang and Stumm, 1973; Hohl and Stumm, 1976; Noh and Schwarz, 1989; Sprycha, 1989). Mica is negatively charged at all pH values. Consequently, above pH 8.1, a repulsive electrostatic force is expected as both surfaces bear surface charges of the same sign. At pH 8.1, a repulsive force was observed as expected for a neutral tip on a charged surface. Compared to the curves shown in Fig. 2, a strong attractive component can be seen. With alumina strong attractive vdW forces were generally measured. From Eq. 1 follows that the electrostatic force should become attractive for

$$\sigma_T^2 + \sigma_S^2 < 2|\sigma_T| \cdot |\sigma_S|,$$

and if σ_T and σ_S are of opposite sign. This was observed below pH 8.1.

Measuring hydration forces

Fig. 5 shows force versus distance curves obtained at different concentration of $MgCl_2$ with a silicon nitride tip on mica. At 3 mM $MgCl_2$ the electrostatic repulsion can be seen. It becomes negligible at higher concentrations of the divalent salt and the vdW attraction dominates. At 3 M $MgCl_2$, again, a repulsive force was measured. It had a decay length of 3 nm and was ~0.07 nN strong. The same behavior was also observed with $CaCl_2$ and $SrCl_2$, where a repulsive force was present at 5-M salt concentration whereas the vdW attraction dominated at 0.5 M. At 3 M KCl no repulsion was observed.

This repulsion is probably due to hydration forces. At concentrations >1 M, the electrostatic repulsion, of Debye length ~0.1 nm, can be completely ignored. In

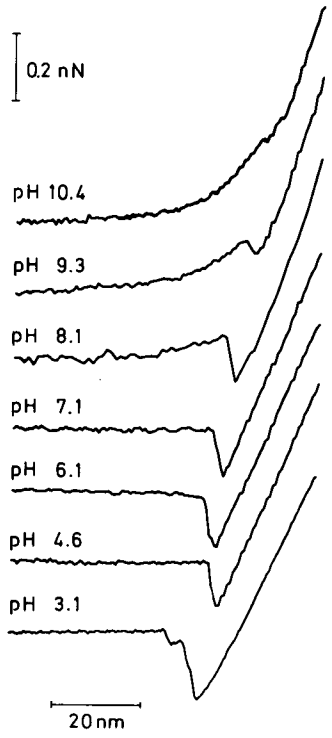

FIGURE 4 Force vs distance curves obtained at different pH values with an alumina tip on mica. The solutions contained 2 mM KCl plus 1 mM of the appropriate buffer. The curves were four times averaged. Only the approach of the sample to the tip is shown.

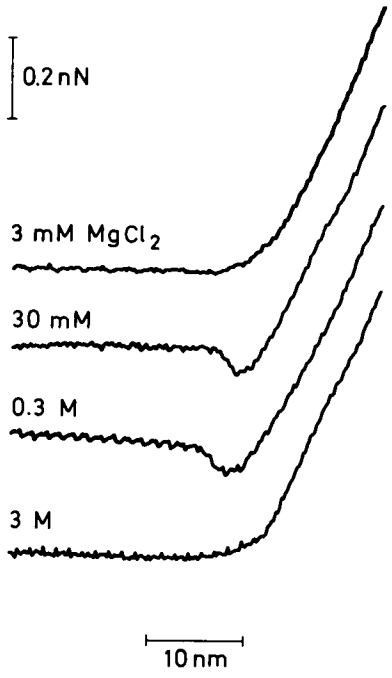

FIGURE 5 Force vs distance curves obtained at different $MgCl_2$ concentrations with a silicon nitride tip on mica (pH ≈ 6). The curves were 16 to 24 times averaged. Only the approach of the sample to the tip is shown.

addition, the force was observed under the same conditions, Pashley and Israelachvili (Pashley, 1981*a* and *b*; Israelachvili and Pashley, 1983; Pashley and Israelachvili, 1984) observed the hydration force (>1 M of divalent cations) and the measured decay length agrees with the one reported by Pashley, 1981 (1.8 nm). Pashley and Israelachvili explained the repulsion as follows. Divalent cations adsorb to the surfaces and bind few layers of water. When the surfaces approach each other the cations have to be dehydrated which increases the free energy of the system and causes a repulsive force. At high concentrations of K^+ also a repulsive hydration force should be present but the decay length is smaller than with divalent cations. Hence, it was probably too small to be detected in my experiments.

Consequences and perspectives

To obtain high resolution images AFMs are usually operated in the contact mode, where the tip is supposed to be touching the surface. Therefore, the externally applied spring force has to overcome the repulsive forces. Hence, the electrostatic and hydration repulsion determine the minimal force that has to be applied. The electrostatic repulsion can be reduced by imaging in salt concentrations > ~50 nm of a monovalent salt. Thus, if the sample is soft or fragile and might be deformed or damaged, the electrolyte should contain 50–100 mM salt. Hydration forces are probably more difficult to eliminate. Though the experiments were done in extreme salt concentrations to make hydration forces visible, hydration forces are probably always present. Positively charged groups like amino groups and cations bound to the sample surface are hydrated and this hydration shell repels the tip.

It has been demonstrated that, in addition to the vdW force, electrostatic and hydration forces can be measured in electrolyte solution with the AFM. As these are also the forces which determine the interaction of colloidal particles (Prost and Rondelez, 1991), the AFM might help to study the behavior of colloids. Interfacial forces have been measured directly for several materials (for a review see Derjaguin et al., 1978, and Israelachvili and McGuiggan, 1988). However, the roughness of the two interacting surfaces usually prevented force measurements for distances <50 nm. Tabor et al. (1969) therefore used thin sheets of molecularly smooth mica glued to glass cylinders of 1-cm radius. The force between these mica cylinders could be measured down to atomic distances (Israelachvili and Adams, 1972). Also, the force between lipid layers deposited onto mica was measured (Marra and Israelachvili, 1985; Marra 1986). Still, force measurements at close distances were restricted to mica or thin layers deposited onto mica. A different approach was chosen by Derjaguin et al., 1977. They realized that the influence of the surface roughness decreases when the interacting surface area decreases. Therefore, they measured the force between cylinders of small radius (0.15–0.5 mm). In this way they could measure interfacial forces down to distances of 15 nm.

With the AFM, the interacting surface area can be further decreased. The tip with a typical radius of curvature of 15 nm interacts only with an area of about the same radius. This fact allows one to investigate the interaction between many different materials as one does not rely on large, molecularly smooth surfaces. The electrostatic force depends on the surface charge density of the sample. Hence, the AFM might be used to measure local surface charge densities. By varying the pH, the point of zero charge might be measured of objects being only ~50 nm large. The main disadvantage of the AFM for measuring surface forces is probably the unknown size and shape of the tip.

I would like to thank E. Bamberg and K. Fendler for their help; C. Noguera, S. Akamine, and A. L. Weisenhorn for discussions; P. Maivald (Digital Instruments) for sending me the program which controlled the slow up and down cycle of the *xyz* translator; R. Petzoldt and H. Volk for excellent drawings and photographs.

This work was supported by the Deutsche Forschungsgemeinschaft Sonderforschungsbereich 169.

Received for publication 31 May 1991 and in final form 16 September 1991.

REFERENCES

Albrecht, T. R. 1989. Advances in atomic force microscopy and scanning tunneling microscopy. Ph.D. thesis, Stanford University, Stanford, California.

Binnig, G., C. F. Quate, and Ch. Gerber. 1986. Atomic force microscope. *Phys. Rev. Lett.* 56:930–933.

Burnham, N. A., and R. J. Colton. 1989. Measuring the nanomechanical properties and surface forces of materials using an atomic force microscope. *J. Vac. Sci. Technol.* A 7:2906–2913.

Burnham, N. A., and R. J. Colton. 1991. Force microscopy. *In* Scanning Tunneling Microscopy: Theory, Techniques, and Applications. D. Bonnell, editor. VCH Publishers. In press.

Burnham, N. A., D. D. Dominguez, R. L. Mowery, and R. J. Colton. 1990. Probing the surface forces of monolayer films with an atomic force microscope. *Phys. Rev. Lett.* 64:1931–1934.

Butt, H.-J. 1991. Electrostatic interaction in atomic force microscopy. *Biophys. J.* In press.

Butt, H.-J., D. N. Wang, P. K. Hansma, and W. Kühlbrandt. 1991. Effect of surface roughness of carbon support films on high-resolution electron diffraction of two-dimensional protein crystals. *Ultramicroscopy.* In press.

Derjaguin, B. V., Y. I. Rabinovich, and N. V. Churaev. 1977. Measurement of forces of molecular attraction of crossed fibres as a function of width of air gap. *Nature (Lond.).* 265:520–521.

Derjaguin, B. V., Y. I. Rabinovich, and N. V. Churaev. 1978. Direct measurement of molecular forces. *Nature. (Lond.)*. 272:313–318.

Girard, C., D. Van Labeke, and J. M. Vigoureux. 1989. Van der Waals force between a spherical tip and a solid surface. *Phys. Rev. B.* 40:12133–12139.

Goodman, F. O., and N. Garcia. 1991. Roles of the attractive and repulsive forces in atomic force microscopy. *Phys. Rev. B.* 43:4728–4731.

Gould, S. A. C., B. Drake, C. B. Prater, A. L. Weisenhorn, S. Manne, G. L. Kelderman, H.-J. Butt, H. Hansma, P. K. Hansma, S. Magonov, and H. J. Cantow. 1990. The atomic force microscope: a tool for science and industry. *Ultramicroscopy.* 33:93–98.

Hartmann, U. 1991. Van der Waals interactions between sharp probes and flat sample surfaces. *Phys. Rev. B.* 43:2404–2407.

Hohl, H., and W. Stumm. 1976. Interaction of Pb^{2+} with hydrous $\gamma - Al_2O_3$. *J. Colloid Interface Sci.* 55:281–288.

Huang, C.-P., and W. Stumm. 1973. Specific adsorption of cations on hydrous $\gamma - Al_2O_3$. *J. Colloid Interface Sci.* 43:409–420.

Israelachvili, J. N. 1985. Intermolecular and Surface Forces. Academic Press, London.

Israelachvili, J. N., and G. E. Adams. 1978. Measurement of forces between two mica surfaces in aqueous electrolyte solutions in the range 0–100 nm. *J. Chem. Soc. Faraday Trans. I.* 74:975–1001.

Israelachvili, J. N., and P. M. McGuiggan. 1988. Forces between surfaces in liquids. *Science (Wash. DC)* 241:795–801.

Israelachvili, J. N., and R. M. Pashley. 1983. Molecular layering of water at surfaces and origin of repulsive hydration forces. *Nature (Lond.)*. 306:249–250.

Lindsay, S. M. 1991. *In* Scanning Tunneling Microscopy: Theory, Techniques, and Applications. D. Bonnell, editor. VCH Publishers. In press.

Marra, J. 1986. Direct measurements of the interaction between phosphatidylglycerol bilayers in aqueous electrolyte solutions. *Biophys. J.* 50:815–825.

Marra, J., and J. N. Israelachvili. 1985. Direct measurement of forces between phosphatidylcholine and phosphatidylethanolamine bilayers in aqueous electrolyte solutions. *Biochemistry.* 24:4608–4618.

Mate, C. M., M. R. Lorenz, and V. J. Novotny. 1989. Atomic force microscopy of polymeric liquid films. *J. Chem. Phys.* 90:7550–7555.

McLaughlin, S. 1977. Electrostatic potentials at membrane-solution interfaces. *In* Current topics in membranes and transport 9. F. Bronner and A. Kleinzeller, editors. Academic Press, New York. 71–144.

Noh, J. S., and J. A. Schwarz. 1989. Estimation of the point of zero charge of simple oxides by mass titration. *J. Colloid Interface Sci.* 130:157–164.

Parsegian, V. A., and D. Gingell. 1972. On the electrostatic interaction across a salt solution between two bodies bearing unequal charges. *Biophys. J.* 12:1192–1204.

Pashely, R. M. 1981*a*. Hydration forces between mica surfaces in aqueous electrolyte solutions. *J. Colloid Interface Sci.* 80:153–162.

Pashely, R. M. 1981*b*. DLVO and hydration forces between mica surfaces in Li^+, Na^+, K^+, and Cs^+ electrolyte solutions: a correlation of double-layer and hydration forces with surface cation exchange properties. *J. Colloid Interface Sci.* 83:531–546.

Pashely, R. M., and J. N. Israelachvili. 1984. DLVO and hydration forces between mica surfaces in Mg^{2+}, Ca^{2+}, Sr^{2+}, and Ba^{2+} chloride solutions. *J. Colloid Interface Sci.* 97:446–455.

Prost, J., and F. Rondelez. 1991. Structures in colloidal physical chemistry. *Nature (Lond.)*. (Suppl.) 350:11–23.

Sprycha, R. 1989. Electric double layer at alumina/electrolyte interface. *J. Colloid Interface Sci.* 127:1–11.

Tabor, D., F. R. S. Winterton, and R. H. S. Winterton. 1969. The direct measurement of normal and retarded van der Waals forces. *Proc. R. Soc. Edinb. Sect. A (Math. Phys. Sci.)* 312:435–450.

Weisenhorn, A. L., P. K. Hansma, T. R. Albrecht, and C. F. Quate. 1989. Forces in atomic force microscopy in air and water. *Appl. Phys. Lett.* 54:2651–2653.

Weisenhorn, A. L., P. Maivald, H.-J. Butt, and P. K. Hansma. 1991. Measuring adhesion, attraction, and repulsion between surfaces in liquids with an atomic force microscope. *Phys. Rev. B.* In press.

Wickramasinghe, H. K. 1989. Scanned-probe microscopes. *Sci. Am.* 260; 10:98–105.